



Review

Bonding capabilities of imidazol-2-ylidene ligands in group-10 transition-metal chemistry

Udo Radius^{a,*}, F. Matthias Bickelhaupt^{b,*,1}^a Institut für Anorganische Chemie der Universität, Engesserstr., Geb. 30.45, D-76128 Karlsruhe, Germany^b Department of Theoretical Chemistry and Amsterdam Center for Multiscale Modeling, Scheikundig Laboratorium der Vrije Universiteit, De Boelelaan 1083, NL-1081 HV Amsterdam, The Netherlands

Contents

1. Introduction	678
2. Bonding in TM–NHC complexes: a brief overview	679
3. Methods	680
3.1. Computational details	680
3.2. Bond analysis	680
3.3. Analysis of the charge distribution	680
4. Results and discussion	681
4.1. Electronic structure of NHC and other ligands	681
4.2. Ni–NHC bonding	682
4.3. Effect of transition metal on M–NHC bonding	683
4.4. Effect of nitrogen substituent on M–NHC bonding	683
4.5. Effect of metal–complex fragment on M–NHC bonding	684
5. Conclusions	685
Acknowledgements	685
References	685

ARTICLE INFO

Article history:

Received 12 March 2008

Accepted 30 May 2008

Available online 8 June 2008

Keywords:

Bond theory

Coordination complexes

Density functional calculations

Group-10 metals

N-heterocyclic carbenes

ABSTRACT

In this contribution, we give a brief overview of studies on the bonding between transition metals (TM) and N-heterocyclic carbenes (NHC) and report on a systematic bond analysis of the bonding of 1,3-diorganyl-imidazol-2-ylidenes (R_2Im) in a series of nickel, palladium and platinum complexes D_{2h} - and D_{2d} - $M(H_2Im)_2$ to exemplify the dependence of the TM–NHC bonding on the group-10 transition metal. Furthermore complexes with seemingly different complex fragment group electronegativities, i.e., $[Ni(R_2Im)_3]$, $[Ni(R_2Im)_2]$, $[Ni(R_2Im)(CO)]$, $[Ni(R_2Im)(CO)_2]$, and $[Ni(R_2Im)(CO)_3]$ have been analyzed, a series that provides theoretical evidence that the bonding of 1,3-diorganyl-imidazol-2-ylidene ligands to metal–complex fragments strongly depends on the nature of the ligand environment. Our results confirm the currently accepted idea that NHCs are not pure σ -donors. In the series of complexes examined here π -contribution is at least 10% and up to 40%, depending on the transition metal complex fragment bonded to the carbene. The dependence of the bonding mechanism on the R substituent in R_2Im has also been investigated.

© 2008 Elsevier B.V. All rights reserved.

1. Introduction

Over the last decades, N-heterocyclic carbenes (NHCs; 1,3-diorganyl-imidazol-2-ylidenes, R_2Im) have evolved from elusive intermediates for which only indirect evidence could be provided [1] to stabilized forms that are currently investigated in many research groups [2]. The isolation of thermally stable N-heterocyclic carbenes by Arduengo et al. in 1991 initiated intense research activ-

* Corresponding author. Tel.: +49 721 6082855; fax: +49 721 6087021.

E-mail addresses: radius@aoc1.uni-karlsruhe.de (U. Radius),fm.bickelhaupt@few.vu.nl (F.M. Bickelhaupt).¹ Tel. +31 20 5987617; fax: +31 20 5987629.

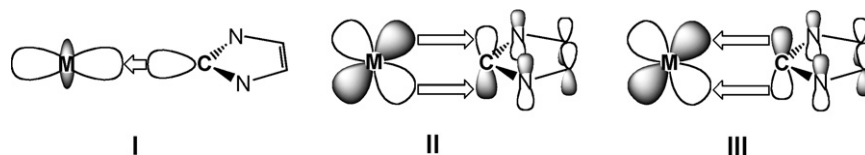


Fig. 1. Important orbital interactions between H_2Im and a transition metal M.

ity into the organometallic chemistry of these versatile ligands. There has been considerable interest in N-heterocyclic carbenes as spectator ligands in organometallic chemistry, particularly as alternatives to phosphine ligands in the field of homogeneous catalysis [3]. Specifically, NHCs have a greater thermal and air stability and lower toxicity, making them ideal candidates for catalysis. The vast majority of reported transition metal (TM) NHC complexes in catalysis have been utilized in olefin metathesis [4] or in palladium catalyzed coupling chemistry [5]. The success story of NHCs in these areas contributed to the wide use of NHC for a diverse set of other catalytic transformations [3]. Thus, NHC have become ubiquitous ligands in organometallic chemistry and catalysis. Nevertheless, the bonding of NHCs to transition metals is still not fully understood [6].

It was generally assumed that NHCs have bonding properties similar to electron-rich trialkylphosphanes (strong σ donors with negligible π -accepting ability) [2,3]. This belief arose mainly from theoretical studies of the electronic structure of NHCs, which assigned a strong N–C(carbene) π -donation as the main reason for the high kinetic stability of this class of compounds [7]. This interaction leads to a high occupancy of the formally unoccupied carbene carbon $p(\pi)$ orbital and there is thus no need for TM–NHC back donation to stabilize the complex. In a number of papers, it has been shown that the ligand-binding energies of NHC are usually larger compared to trialkylphosphines [2,3,6]. To assess the M–C orbital interaction in TM–NHC complexes completely, three interactions might be of relevance (see Fig. 1): (a) σ donation I from the NHC σ -donor orbital to a TM acceptor orbital, (b) π -backdonation II from an occupied TM d_{π} orbital into the NHC carbon p_{π} orbital, and (c) delocalization of the NHC π -system into an unoccupied TM d_{π} (or p_{π} , not shown) orbital, i.e., π donation III.

2. Bonding in TM–NHC complexes: a brief overview

In the last few years, several theoretical studies have suggested various degrees of π -bonding in TM–NHC complexes [6]. In a first theoretical analysis on complexes of the type $[(NHC)MX]$ ($M = Cu, Ag, Au$), Frenking et al. [6b] demonstrated that the TM–NHC bonds have large electrostatic contributions and that the covalent part of the bonding (i.e., orbital interactions) shows negligible π -backbonding from the TM to the NHC ligand. Already in the 1970s, however, Taube and Clarke [6a] reported, in an experimental paper, π -backbonding in carbon bound ruthenium xanthine complexes, and calculations of Lammertsma et al. [6d] on iridium NHC complexes as well as of Meyer et al. on copper, silver and gold NHC complexes [6e,f] led to the conclusion that NHCs are not only excellent σ -donors, but also fair π -acceptor ligands, even for cationic TM d^{10} complexes. According to their work, π -backbonding can be significant with electron-rich metal centers and might contribute up to 20–30% of the orbital interaction. In a more recent computational study in which the bonding in $[(NHC)MX]$ ($M = Cu, Ag, Au$) complexes was reinvestigated [6g], Frenking and co-workers estimate that the orbital interaction part of the bonding has approximately 20% π -backbonding. Furthermore, in this study the authors stated that the metal–carbene bonds are mainly held together by classi-

cal electrostatic attraction, which contributes at least 65% of the binding interactions.

Based on DFT calculations on cyclometallation products of the complexes $[MCl(tBu_2Im)_2]^+$ [6h] ($M = Rh, Ir$), Nolan et al. concluded that the key in understanding the unusual stability of these complexes lies in π -donation of the NHC ligands. One MO of the overall complex responsible for π -interaction seemingly results from a mixing of NHC π (64%) and NHC π^* (3%) orbitals. This was interpreted as to indicate the ability of NHC ligands to act as π -electron donors. This idea was substantiated in a fine paper published by Jacobsen and co-workers just recently [6k], which contributes to the discussion with a systematic analysis of TM–NHC bonding in a series of complexes, in which the formal d-electron counts range from d^0 to d^{10} . Their results confirm the idea that NHCs are not pure σ -donors, leading to at least 10% π -contribution. The lowest values have been calculated for early TM complexes and for cationic complexes $[M(H_2Im)(PH_3)]^+$ ($M = Cu, Ag, Au$). These π -interactions are dominated by the backbonding contribution, whose significance increases with increasing d-electron count of the TM. Most interestingly, they also find π -contributions for formally d^0 TM complexes, which accounts for some ligand-to-metal π -donation. In their calculations over a whole range of NHC complexes Jacobsen et al. find a large spectrum of overall TM–NHC bonding energies, ranging from 98 kcal/mol for $[Au(H_2Im)(PH_3)]^+$ to 27 kcal/mol for $[Ti(H_2Im)Cl_5]^-$. They propose that, with the exception of the cationic d^{10} systems $[M(H_2Im)(PH_3)]^+$ ($M = Cu, Ag, Au$), orbital interaction is the dominant bonding contribution in TM–NHC complexes. For the cationic systems, electrostatic interaction constitutes the most important bonding force. Furthermore, they provide evidence that systems with higher formal d-electron count form stronger TM–NHC bonds. Roesler et al. [6m] confirmed these results in a recent theoretical study on the electronic structures and ligand properties of various NHCs with inorganic backbones. Inspection of the nature of the TM–carbene bonds in complexes $[M(NHC)Cl_5]^-$ ($M = Ti, Zr, Hf$), $M(NHC)(CO)_5$ ($M = Cr, Mo, W$) and $M(H_2Im)Cl$ ($M = Cu, Ag, Au$) revealed that π -contribution is moderate to important in all systems studied, ranging from approximately 10% to almost 35% of the total orbital interaction energy. According to their energy decomposition and charge decomposition analyses, the maximum for π -interaction is reached for group-11 metal–NHC complexes, contrarily to the findings of Jacobsen and co-workers.

These recent calculations suggest that NHC ligands in TM complexes exhibit an ambivalent π -bonding character, depending on the metal-complex fragment coordinated to the carbene. Therefore, we wish to provide a detailed account on the bonding of NHC ligands binding to metal-complex fragments mainly of the same metal (nickel) with seemingly different complex-fragment group electronegativities. We aim to provide here a deeper understanding of the nature of the π bonding and its significance for the overall stability of the Ni–NHC coordination bond. We also investigate, for selected examples, the role of the nitrogen substituent (H, Me, *i*Pr, Ph; abbreviations for the NHC ligands used: H_2Im , Me_2Im , iPr_2Im , Ph_2Im) on the Ni–NHC bonding as well as the role of the metal by including palladium and platinum complexes in our set of model

systems. We have chosen Ni–NHC complexes for the present study because of our own research interests and because of a wealth of experimental data, which has been reported for this class of complexes over the last few years. [8–10] This background provides a sound basis for comparing our computational results with experiment.

3. Methods

3.1. Computational details

All calculations are based on density functional theory (DFT) [11] and were carried out using the Amsterdam Density Functional (ADF) program [12,13]. The BLYP density functional was used, [14] in combination with a large uncontracted set of Slater-type orbitals (STOs) containing diffuse functions. This basis set is designated TZ2P: it is of triple- ζ quality and has been augmented with two sets of polarization functions: 2p and 3d on H, 3d and 4f on C and N, 5p and 4f on Pd. The core shells of carbon (1s), fluorine (1s), chlorine (1s2s2p), nickel palladium and platinum; (1s2s2p3s3p3d) were treated by the frozen-core approximation [12]. An auxiliary set of s, p, d, f and g STOs was used to fit the molecular density and to represent the Coulomb and exchange potentials accurately in each SCF cycle [13]. Relativistic effects were accounted for using the zeroth-order regular approximation (ZORA) [15]. Recently, we showed that our approach is in good agreement with high-level *ab initio* benchmarks for oxidative addition reactions [16]. Equilibrium geometries were fully optimized using analytical gradient techniques. All structures were verified to be energy minima through a vibrational analysis.

3.2. Bond analysis

The overall coordination-bond energy ΔE is made up of two major components (Eq (1)):

$$\Delta E = \Delta E_{\text{prep}} + \Delta E_{\text{int}} \quad (1)$$

In this formula, the preparation energy ΔE_{prep} is the amount of energy required to deform the separate bases from their equilibrium structure to the geometry that they acquire in the pair. The interaction energy ΔE_{int} corresponds to the actual energy change when the prepared fragments are combined to form the overall coordination complex. It is analyzed in our model systems in the framework of the Kohn-Sham MO model using a decomposition of the bond into electrostatic interaction, exchange repulsion (or Pauli repulsion), and (attractive) orbital interactions (Eq (2)) [17]:

$$\Delta E_{\text{int}} = \Delta V_{\text{elstat}} + \Delta E_{\text{Pauli}} + \Delta E_{\text{oi}} \quad (2)$$

The term ΔV_{elstat} corresponds to the classical electrostatic interaction between the unperturbed charge distributions of the prepared (i.e., deformed) fragments and is usually attractive. The Pauli-repulsion ΔE_{Pauli} comprises the destabilizing interactions between occupied orbitals and is responsible for the steric repulsion. The orbital interaction ΔE_{oi} in any MO model, and therefore also in Kohn-Sham theory, accounts for charge transfer (i.e., donor–acceptor interactions between occupied orbitals on one moiety with unoccupied orbitals of the other, including the HOMO–LUMO interactions) and polarization (empty/occupied orbital mixing on one fragment due to the presence of another fragment). Since the Kohn-Sham MO method of DFT in principle yields exact energies and, in practice, with the available density functionals for exchange and correlation, rather accurate energies, we have the special situation that a seemingly one-particle model (an MO method) in principle completely accounts for the bonding energy [18a].

The orbital interaction energy can be decomposed into the contributions from each irreducible representation Γ of the interacting system (Eq. (3)) using the extended transition state (ETS) scheme developed by Ziegler and Rauk [18]:

$$\Delta E_{\text{oi}} = \sum_{\Gamma} \Delta E_{\Gamma} \quad (3)$$

Note that our approach differs in this respect from the Morokuma scheme [19], which instead attempts a decomposition of the orbital interactions into polarization and charge transfer. In systems with a clear σ/π separation, the above symmetry partitioning proves to be most informative.

3.3. Analysis of the charge distribution

The electron density distribution is analyzed using the Voronoi deformation density (VDD) method [20]. The VDD charge Q_A is computed as the (numerical) integral of the deformation density $\Delta\rho(r) = \rho(r) - \sum_B \rho_B(r)$ associated with the formation of the molecule from its atoms over the volume of the Voronoi cell of atom A (Eq. (4)). The Voronoi cell of atom A is defined as the compartment of space bounded by the bond midplanes on and perpendicular to all bond axes between nucleus A and its neighboring nuclei (cf. the Wigner-Seitz cells in crystals) [21].

$$Q_A = - \int_{\text{Voronoi cell A}} (\rho(r) - \sum_B \rho_B(r)) dr \quad (4)$$

Here, $\rho(r)$ is the electron density of the molecule and $\sum_B \rho_B(r)$ the superposition of atomic densities ρ_B of a fictitious promolecule without chemical interactions that is associated with the situation in which all atoms are neutral. The interpretation of the VDD charge Q_A is rather straightforward and transparent. Instead of measuring the amount of charge associated with a particular atom A, Q_A directly monitors how much charge flows, due to chemical interactions, out of ($Q_A > 0$) or into ($Q_A < 0$) the Voronoi cell of atom A, that is, the region of space that is closer to nucleus A than to any other nucleus.

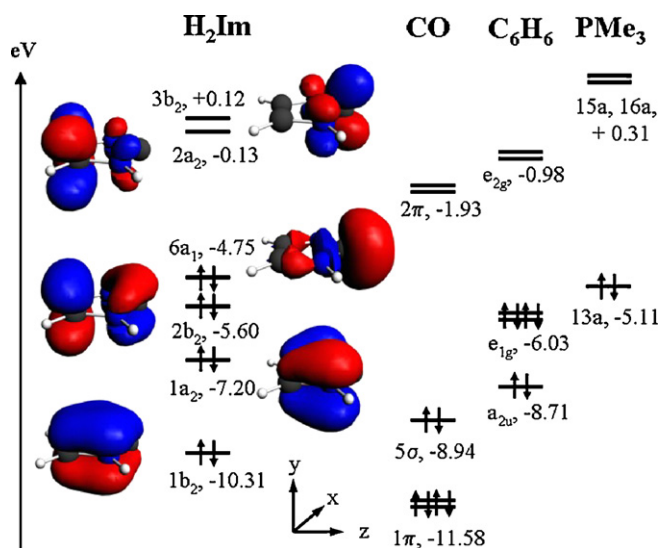


Fig. 2. Comparison of frontier orbitals and orbital energies (in eV) of imidazol-2-ylidene (H_2Im), CO, C_6H_6 and PMe_3 .

4. Results and discussion

4.1. Electronic structure of NHC and other ligands

Our purpose is to discuss TM–NHC bonding in electron-rich d^{10} nickel complexes. It is instructive to preface our analysis of the complexes with some considerations emerging from the free ligand. Therefore, we recall the main electronic features of the parent imidazol-2-ylidene H_2Im . Important orbitals of H_2Im emerging from our DFT calculations are given in Fig. 2 as well as a comparison of the orbital energies with two ubiquitous ligands in organometallic chemistry, the carbonyl and the benzene ligand.

Shortly after the discovery of stable singlet carbenes by Arduengo et al. [22], a number of theoretical papers appeared which presented models for the bonding and structure in imidazol-2-ylidenes and diaminocarbenes in general [7]. It has been shown that the groundstate electron distribution in imidazol-2-ylidenes reflects a remarkable similarity to those in some of the more classical 1A_1 carbenes, such as CF_2 , and it seems now to be generally accepted that two main effects are responsible for the stabilization of singlet carbenes in comparison with triplet carbenes, that is σ -polarization and π -donation. The polarization of the electron pairs located in the bond between the carbene carbon atom and its neighbor atoms can be achieved by the introduction of electronegative substituents X at the carbene carbon atom. This leads to an increase of p-character in the C–X bond and an increase of s-character in the carbene σ -sp orbital and thus to a lowering of the orbital energy of the σ -orbital. The second effect is π -donation from a heteroatom X attached to the carbene carbon into the carbene carbon p orbital, which leads – in terms of molecular orbitals – to an occupied combination with large contributions on the heteroatom and an unoccupied combination with large contribution of the carbene carbon p orbital. Both effects lead to an energy gap between σ - and π -orbital, which is large enough to lead to a singlet groundstate.

In the case of imidazol-2-ylidenes, the electrons responsible for π -interaction are embedded into a 6 electron π -aromatic system at the five membered ring. These π -orbitals along with the corresponding orbital energies are shown in Fig. 2. Similarly to the well known cyclopentadienide anion, the occupied orbitals have no nodal plane (orbital $1b_2$ in C_{2v} symmetry, at -10.31 eV) or one nodal plane ($1a_2$, -7.20 eV and $2b_2$, -5.60 eV), whereas the unoccupied π -orbitals ($2a_2$, -0.13 eV and $3b_2$, $+0.12$ eV) have two nodal planes. These pairs of orbitals are not degenerate due to the heterosubstitution of the aromatic ring. The HOMO of the NHC is the orbital $6a_1$ at -4.75 eV, which contains 49.5% p_z and 33.5% s of the carbene carbon atom as main contributions. The orbital $3b_2$ is also mainly centered on the carbene carbon atom with 71.4% p_y . We calculate an energy gap of 4.87 eV between these two important carbon-centered orbitals. When it comes to TM–NHC binding in the z direction, orbital $6a_1$ is responsible for σ -bonding, whereas an interaction of $3b_2$ with metal centered orbitals of the appropriate symmetry can lead to π -backdonation.

Before entering into the analysis of a TM–NHC bond, it is worth to take also the other orbitals of the π -system into consideration. Orbitals of a_2 symmetry have no contributions of the carbene carbon atom, but $1b_2$ and $2b_2$ have carbene carbon p_y contributions of 13.2% ($1b_2$) and 20.0% ($2b_2$), respectively. Whereas the orbital $1b_2$ is too low in energy to play an important role in TM–NHC binding, the orbital $2b_2$ might be well suited for some π -donation. As a comparison, energy levels for the orbitals of CO and C_6H_6 which are important for a description of TM–CO and TM– C_6H_6 bonding are also given in Fig. 2. The unoccupied 2π acceptor orbitals of CO [23] are energetically much lower (at -1.93 eV at our level of theory, containing approximately 76% C 2p) compared to H_2Im 's $3b_2$, a

strong indication that CO is indeed the much better π -acceptor ligand. The π -donation properties of CO are usually neglected, since the 1π orbital of CO is low in energy and there is only a small contribution of CO carbon p orbital to these MOs [23]. Using the same method as for the calculations of H_2Im , we calculate the CO energy levels 1π at -11.58 eV with a carbon p contribution of roughly 25 (24.7%). On the other side, the importance of δ contributions to the bonding of arenes in metal arene complexes such as bisbenzene chromium is well established [24] and the energy calculated for the C_6H_6 e_{2g} orbitals is in a similar energetic region (-0.98 eV) as the orbital $3b_2$ of H_2Im . Interestingly, the importance of π contributions to arene TM bonding is also well documented (approximately 15% for bisbenzene chromium according to Ref. [24]) and the energy calculated for the C_6H_6 e_{1g} orbitals is in the same energetic region (-6.03 eV) as the orbital $2b_2$ of H_2Im . However, in the case of C_6H_6 this orbital is exclusively built up from carbon p orbitals, which are excellently directed to the metal atom. For further comparison, we also calculated PMe_3 as a typical electron rich phosphine and obtained an energy of -5.11 eV for the lone pair, indicative for earlier predicted and experimentally observed better donor properties of NHCs as compared to PMe_3 .

Following Fukui's frontier orbital concept [25], imidazol-2-ylidenes should therefore be regarded as excellent σ -donor ligands with π -acceptance properties (although much worse than those

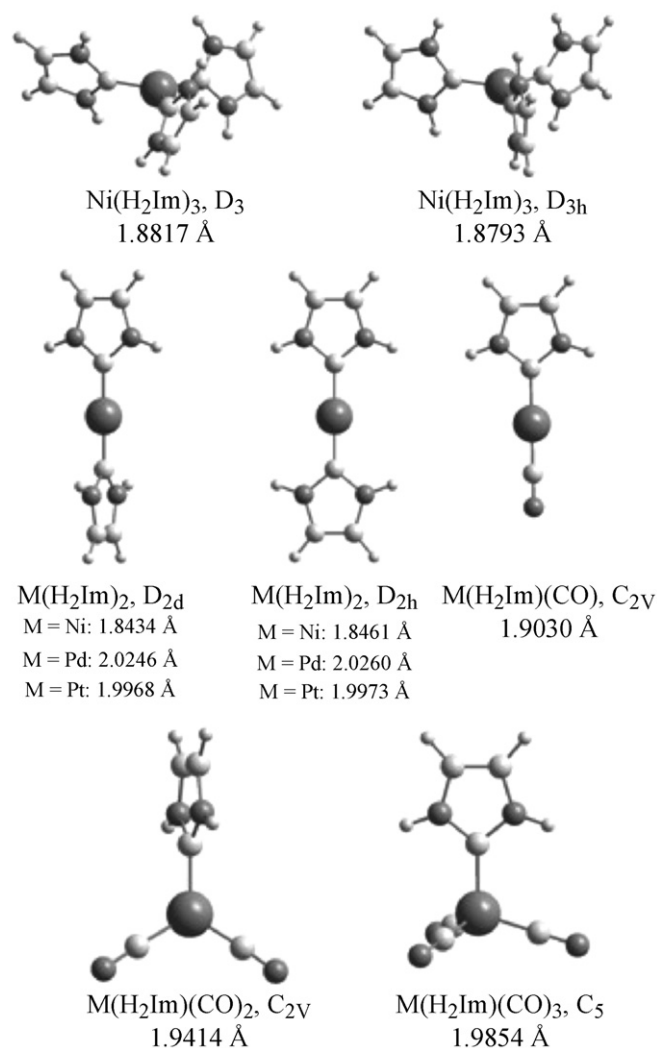


Fig. 3. Structures of our model complexes with M–C(carbene) distances.

of CO) as well as ligands with π -donating properties, depending on the nature of the transition metal complex fragment which is coordinated to the NHC ligand.

4.2. Ni–NHC bonding

For an analysis of TM–NHC bonding in dependence of the nature of the metal-complex fragment, we chose to first analyze models of known nickel complexes. Electron-rich NHC nickel complexes are amongst the first NHC metal compounds that have been synthesized starting from isolated N-heterocyclic carbenes [8a]. Starting from $\text{Ni}(\text{COD})_2$ and sterically demanding, aryl substituted carbene ligands, two-fold coordinated, homoleptic complexes of the type $\text{Ni}(\text{NHC})_2$ have been synthesized in the groups of Arduengo and Herrmann, respectively, namely, $\text{Ni}(\text{Mes}_2\text{Im})_2$ [8a] ($\text{Mes} = 2,3,5\text{-Me}_3\text{C}_6\text{H}_2$) and $\text{Ni}(\text{Dip}_2\text{Im})_2$ [8b] ($\text{Dip} = 2,5\text{-iPr}_2\text{C}_6\text{H}_3$). Cloke et al. reported the synthesis of the alkyl substituted $\text{Ni}(\text{tBu}_2\text{Im})_2$ in 10% yield via co-condensation reaction of nickel vapor and 1,3-di(*tert*-butyl)imidazol-2-ylidene [8c]. We have shown just recently that the outcome of the reaction of $\text{Ni}(\text{COD})_2$ with alkyl-substituted carbenes critically depends on the steric demand of the nitrogen substituent [10]. In the case of the reaction with an isopropyl substituted carbene, the dinuclear complex $\text{Ni}_2(\text{iPr}_2\text{Im})_4(\text{COD})$ is formed as main product, whereas the reaction with the methyl substituted carbene afforded exclusively homoleptic three-fold substituted $\text{Ni}(\text{Me}_2\text{Im})_3$ [10b]. These types of homoleptic complexes seem to be ideal for our purpose to analyze Ni–NHC bonding, since they contain only the metal and imidazol-2-ylidene ligands. To avoid any steric influence we performed these calculations on reduced models of the complexes of the type $\text{Ni}(\text{NHC})_2$ and $\text{Ni}(\text{NHC})_3$, i.e., $\text{Ni}(\text{H}_2\text{Im})_2$ and $\text{Ni}(\text{H}_2\text{Im})_3$. An overview of the model complexes under investigation along with calculated metal carbon distances of the optimized structures is given in Fig. 3. All the compounds

have been optimized without any symmetry constraints as well as under symmetry restrictions.

The experimentally observed trends in M–C bond lengths in complexes of the type $\text{M}(\text{NHC})_2$ is well reproduced by our calculations (see Fig. 3). X-ray crystal structures of the nickel complexes reveal Ni–C bond lengths of 1.827 Å and 1.830 Å for $\text{Ni}(\text{Mes}_2\text{Im})_2$ [8a], and 1.874 Å for $\text{Ni}(\text{tBu}_2\text{Im})_2$ [8c]. The Pt–C distances in the solid-state structure of $\text{Pt}(\text{Mes}_2\text{Im})_2$ were found to be 1.942 and 1.952 Å [8a], and the Pd–C distances of three X-ray analyses on different palladium complexes $\text{Pd}(\text{R}_2\text{Im})_2$ are in a range between 1.990 and 2.084 Å [8d–f]. We calculate the shortest M–C distances for nickel complexes (e.g., 1.8461 Å for $D_{2h}\text{-Ni}(\text{H}_2\text{Im})_2$) and the longest for the palladium complexes (e.g., 2.0260 Å for $D_{2h}\text{-Pd}(\text{H}_2\text{Im})_2$). The computed Pt–C bond distances (e.g., 1.9973 Å for $D_{2h}\text{-Pt}(\text{H}_2\text{Im})_2$) are slightly shorter than the corresponding Pd–C distances (e.g., 2.0260 Å for $D_{2h}\text{-Pd}(\text{H}_2\text{Im})_2$).

For simplicity, we want start our analysis of the bonding with complexes of the type $\text{Ni}(\text{NHC})_2$, but not with the experimentally observed rotamers of pseudo D_{2d} symmetry, but with the D_{2h} symmetric molecule, i.e., $D_{2h}\text{-Ni}(\text{H}_2\text{Im})_2$. This optimized molecule is a transition state for the twist of the ligands to give the D_{2d} symmetric molecule, but it is only 0.61 kcal/mol higher in energy than $D_{2h}\text{-Ni}(\text{H}_2\text{Im})$. A schematic frontier orbital interaction diagram for the interaction of the metal atom with two H_2Im ligands is given in Fig. 4. On the left side of Fig. 4 the orbitals are shown of the two NHC ligands separated by 3.6922 Å. In principle, this part reveals exactly the orbital introduced for H_2Im twice, since for each orbital a symmetric and antisymmetric combination has now to be considered. On the right side of Fig. 4, the nickel 3d, 4s, and 4p orbitals are shown, labeled according to D_{2h} symmetry. When the interaction between these two fragments is switched on, there is significant orbital overlap between the orbitals of a_g , b_{2u} , and b_{3g} symmetry. The interaction of ligand $1a_g$ orbital with nickel d_{z^2} and s leads to a σ -type orbital $1a_g$ of the complex. Similarly, ligand $1b_{2u}$ has

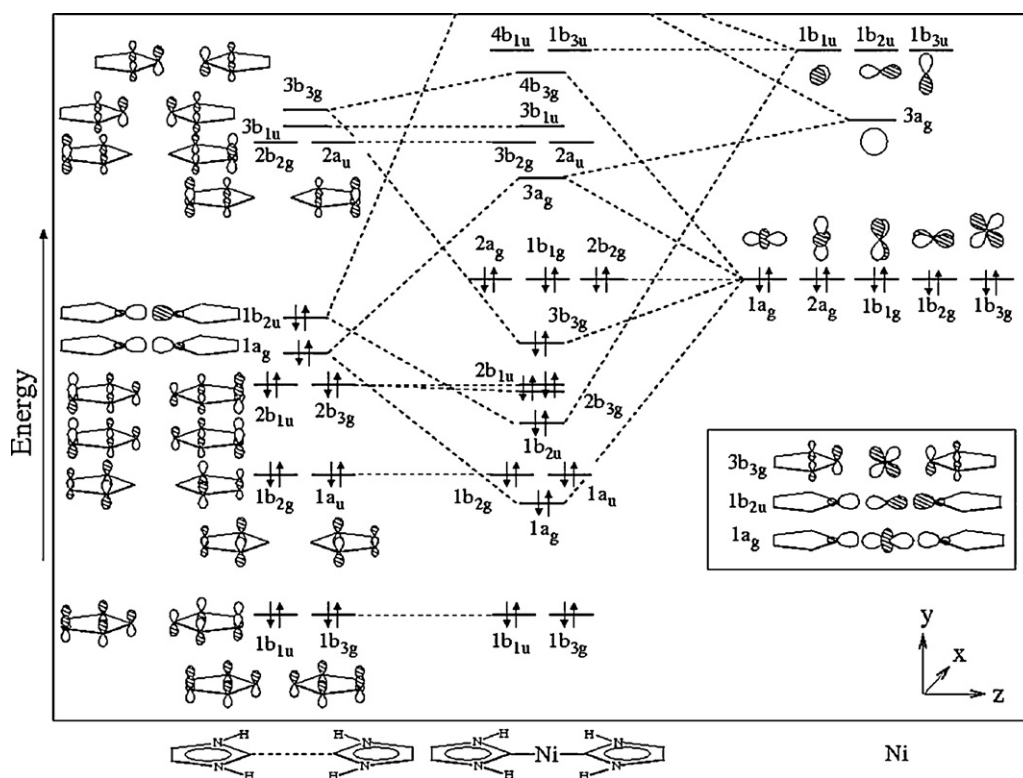


Fig. 4. Schematic orbital-interaction diagram for a fragment consisting of two imidazol-2-ylidenes (left side) binding to a nickel atom (right side) yielding $D_{2h}\text{-Ni}(\text{H}_2\text{Im})_2$.

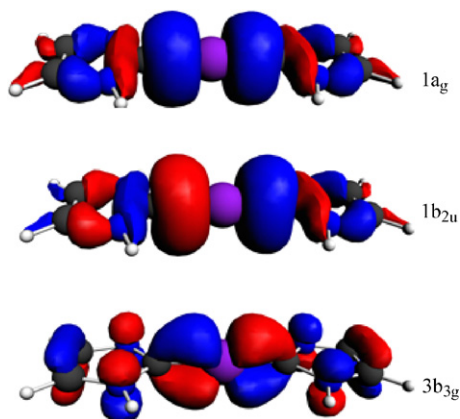


Fig. 5. 3D plots of important σ - and π -bonding orbitals of D_{2h} -Ni(H₂Im)₂.

the right symmetry to interact with nickel p_z to form another σ -bonding orbital. For π interaction, the b_{3g} orbitals of the ligand have the right symmetry to interact with nickel d_{yz} . Ligand orbital $1b_{3g}$ is too low in energy for efficient interaction, but the occupied orbital $2b_{3g}$ and the unoccupied orbital $3b_{3g}$ interact significantly with nickel d_{yz} . Whereas interaction of $2b_{3g}$ and the occupied nickel $d^{10} d_{yz}$ orbital leads to π -repulsion, the interaction of unoccupied $2b_{3g}$ and the occupied nickel $d^{10} d_{yz}$ is a strong bonding interaction. The highest occupied orbitals of the complex are the nickel centered d orbitals $2a_g$ (d_{xy}), $1b_{1g}$ ($d_{x^2-y^2}$), and $2b_{2g}$ (d_{xz}).

Summarizing, three orbitals of D_{2h} -Ni(H₂Im) are mainly responsible Ni–NHC bonding. These are the σ -type orbitals $1a_g$ (in D_{2h} symmetry) and $1b_{2u}$, which represent the two σ -bonds in the molecule, and the π -interaction $3b_{3g}$, representing a π -bond in the molecule. These orbitals are shown schematically in the box on the right side of Fig. 4 and plots of these orbitals are provided in Fig. 5.

The importance of nickel–carbon π -backbonding in this type of complex was substantiated by the energy decomposition of the Ni–C_{carbene} orbital interaction of the two fragments Ni(H₂Im) and H₂Im in C_{2v} symmetry (see Table 1). Out of a total orbital interaction of -47.06 kcal/mol, -22.83 kcal/mol stem from interaction of a_1 symmetry (i.e., σ -contribution), -16.92 kcal/mol from

interaction of b_2 symmetry (i.e., π -contribution), -7.31 kcal/mol from interactions of a_2 and b_1 symmetry (i.e., interaction of nickel-centered orbitals with the σ -frame of the carbene). For this complex, π bonding contributes as much as 36% to the net orbital interaction. This value even increases up to 43% for D_{2d} -Ni(H₂Im)₂, a model for the experimentally observed complexes Ni(R₂Im)₂. Note how important orbital interaction of the carbene carbon atom with the metal atom is, in this case, since it contributes -47.06 kcal/mol (D_{2h} -Ni(H₂Im)₂) and -48.55 kcal/mol (D_{2d} -Ni(H₂Im)₂), respectively, to the overall coordination-bond energy ΔE of -50.19 kcal/mol (D_{2h} -Ni(H₂Im)₂) and -51.59 kcal/mol (D_{2d} -Ni(H₂Im)₂). Without this contribution the complexes would be hardly bound at all.

4.3. Effect of transition metal on M–NHC bonding

The amount of π -backbonding also critically depends on the nature of the metal atom involved in TM–NHC bonding: For Pd- and Pt-complexes of the type D_{2d} -M(H₂Im)₂ (M = Pd, Pt), we calculate 30 and 26% π -contribution to the total orbital interaction, strongly reduced as compared to 43% obtained for the corresponding nickel complex. For the overall coordination-bond energy ΔE , we recognize a trend typically observed for bonding energies within a group of metals, i.e., a minimum for the 4d metal palladium: [26] -51.59 kcal/mol (Ni), -43.27 kcal/mol (Pd), and -54.86 kcal/mol (Pt). The analyses of the present series of model systems show that the decrease in bonding interaction from the nickel to the palladium compound mainly originates from a reduced π -backdonation whereas the *strengthening* from the palladium to the platinum compound is associated with a much more favorable σ -orbital interaction for the heaviest congener. Note, however, also that it is especially the sharp increase of the electrostatic attraction from the palladium to the platinum complex that contributes to the concomitant increase in overall TM–NHC bond strength.

4.4. Effect of nitrogen substituent on M–NHC bonding

To investigate the dependence of the Ni–NHC bonding on the nitrogen substituent of the carbene ligand, we analyzed

Table 1
Metal–carbene bond energy decomposition (in kcal/mol) for complexes M(H₂Im)₂ (M = Ni, Pd, Pt)^a

	Ni(H ₂ Im) ₂ $D_{2d}(C_{2v})$	Ni(H ₂ Im) ₂ $D_{2h}(C_{2v})$	Pd(H ₂ Im) ₂ $D_{2d}(C_{2v})$	Pd(H ₂ Im) ₂ $D_{2h}(C_{2v})$	Pt(H ₂ Im) ₂ $D_{2d}(C_{2v})$	Pt(H ₂ Im) ₂ $D_{2h}(C_{2v})$
Decomposition of orbital interactions ^b						
σ	–21.86	–22.83	–23.44	–23.47	–38.90	–38.95
π	–20.94	–16.92	–11.92	–11.17	–16.31	–15.26
Other	–5.75	–7.31	–4.32	–4.61	–6.68	–7.14
ΔE_{oi}	–48.55	–47.06	–39.69	–39.26	–61.89	–61.35
% π to ΔE_{oi}	43.1	36.0	30.0	28.4	26.4	24.9
Decomposition of interaction energy ^c						
ΔE_{oi}	–48.55	–47.06	–39.69	–39.26	–61.89	–61.35
ΔE_{Pauli}	137.81	136.84	136.52	135.89	197.41	196.97
ΔV_{elstat}	–143.46	–142.67	–141.36	–140.73	–195.33	–194.97
ΔE_{int}	–54.21	–52.89	–44.52	–44.10	–59.81	–59.35
Decomposition of overall bond energy ^d						
ΔE_{int}	–54.21	–52.89	–44.52	–44.10	–59.81	–59.35
$\Delta E_{prep}(ML_n)$	+2.23	+2.35	+1.01	+1.05	4.57	4.62
$\Delta E_{prep}(L)$	+0.39	+0.35	+0.24	+0.23	0.38	0.37
ΔE	–51.59	–50.19	–43.27	–42.82	–54.86	–54.31

^a Computed at BLYP/TZ2P.

^b $\Delta E_{oi} = \Delta E_{oi}(\Gamma_1) + \Delta E_{oi}(\Gamma_2) + \dots$

^c $\Delta E_{int} = \Delta E_{oi} + \Delta V_{elstat} + \Delta E_{Pauli}$.

^d $\Delta E = \Delta E_{int} + \Delta E_{prep}(ML_n) + \Delta E_{prep}(L)$.

Table 2
Metal–carbene bond energy decomposition (in kcal/mol) of complexes $\text{Ni}(\text{R}_2\text{Im})_2^a$

	$\text{Ni}(\text{H}_2\text{Im})_2$ $D_{2d}(\text{C}_{2v})$	$\text{Ni}(\text{H}_2\text{Im})_2$ $D_{2h}(\text{C}_{2v})$	$\text{Ni}(\text{Me}_2\text{Im})_2$ $D_{2d}(\text{C}_{2v})$	$\text{Ni}(\text{Me}_2\text{Im})_2$ $D_{2h}(\text{C}_{2v})$	$\text{Ni}(\text{iPr}_2\text{Im})_2$ $D_{2d}(\text{C}_{2v})$	$\text{Ni}(\text{iPr}_2\text{Im})_2$ $D_{2h}(\text{C}_{2v})$	$\text{Ni}(\text{Ph}_2\text{Im})_2$ $D_{2d}(\text{C}_{2v})$
Decomposition of orbital interactions ^b							
σ	–21.86	–22.83	–23.95	–24.86	–25.29	–25.91	–21.52
π	–20.94	–16.92	–20.00	–16.55	–19.58	–16.53	–21.76
Other	–5.75	–7.31	–7.04	–8.77	–7.61	–9.39	–7.50
ΔE_{oi}	–48.55	–47.06	–50.99	–50.18	–52.48	–51.84	–50.78
% π to ΔE_{oi}	43.1	35.9	39.2	32.9	37.3	31.9	42.9
Decomposition of interaction energy ^c							
ΔE_{oi}	–48.55	–47.06	–50.99	–50.18	–52.48	–51.84	–50.78
ΔE_{Pauli}	137.81	136.84	145.47	143.56	150.00	148.25	137.24
ΔV_{elstat}	–143.46	–142.67	–148.02	–144.82	–150.72	–147.69	–139.08
ΔE_{int}	–54.21	–52.89	–53.55	–51.55	–53.20	–51.27	–52.61
Decomposition of overall bond energy ^d							
ΔE_{int}	–54.21	–52.89	–53.55	–51.55	–53.20	–51.27	–52.61
$\Delta E_{\text{prep}}(\text{ML}_n)$	2.23	2.35	2.07	2.41	1.97	2.30	2.01
$\Delta E_{\text{prep}}(\text{L})$	0.39	0.35	0.36	0.37	0.37	0.37	5.74
ΔE	–51.59	–50.19	–51.12	–48.77	–50.86	–48.60	–44.86

^a Computed at BLYP/TZ2P.

^b $\Delta E_{\text{oi}} = \Delta E_{\text{oi}}(\Gamma_1) + \Delta E_{\text{oi}}(\Gamma_2) + \dots$

^c $\Delta E_{\text{int}} = \Delta E_{\text{oi}} + \Delta V_{\text{elstat}} + \Delta E_{\text{Pauli}}$.

^d $\Delta E = \Delta E_{\text{int}} + \Delta E_{\text{prep}}(\text{ML}_n) + \Delta E_{\text{prep}}(\text{L})$.

complexes of the type D_{2h} - and D_{2d} - $\text{Ni}(\text{R}_2\text{Im})_2$ for different substituents R, i. e. in addition to the parent carbene (R=H) complexes with R=Me, iPr, Ph. As a model for the known two-fold homoleptic substituted complexes of aryl substituted carbenes we performed calculations on the compound D_{2d} - $\text{Ni}(\text{Ph}_2\text{Im})_2$, using a phenyl substituent instead of the widely employed mesityl or diisopropylphenyl groups to reduce computational effort. Comparing the alkyl substituted complexes of D_{2d} symmetry, it is evident that the overall coordination-bond energy ΔE slightly decreases, we calculate –51.59 kcal/mol for D_{2d} - $\text{Ni}(\text{H}_2\text{Im})_2$, –51.12 kcal/mol for D_{2d} - $\text{Ni}(\text{Me}_2\text{Im})_2$, and –50.86 kcal/mol for D_{2d} - $\text{Ni}(\text{iPr}_2\text{Im})_2$, whereas the orbital interaction ΔE_{oi} increases in the same row: –48.55 for D_{2d} - $\text{Ni}(\text{H}_2\text{Im})_2$, –50.99 kcal/mol for D_{2d} - $\text{Ni}(\text{Me}_2\text{Im})_2$, and –52.48 kcal/mol for D_{2d} - $\text{Ni}(\text{iPr}_2\text{Im})_2$. This trend can also be observed for complexes of D_{2h} symmetry. We attribute the slight reduction of overall coordination-bond energy ΔE to steric repulsion. The contribution of π -interaction is in this row also slightly reduced. A closer inspection, however, reveals that the orbital interaction emerging from π -symmetry decreases only slightly (–20.94 for D_{2d} - $\text{Ni}(\text{H}_2\text{Im})_2$, –20.00 kcal/mol for D_{2d} - $\text{Ni}(\text{Me}_2\text{Im})_2$, and –19.58 kcal/mol for D_{2d} - $\text{Ni}(\text{iPr}_2\text{Im})_2$), whereas orbital interaction emerging from σ -symmetry increases much more significantly (–21.86 for D_{2d} - $\text{Ni}(\text{H}_2\text{Im})_2$, –23.95 kcal/mol for D_{2d} - $\text{Ni}(\text{Me}_2\text{Im})_2$, and –25.29 kcal/mol for D_{2d} - $\text{Ni}(\text{iPr}_2\text{Im})_2$). Most interesting for us was a comparison of the bonding features of the complexes stabilized with (i) the isopropyl substituted carbene [10] and (ii) the phenyl substituted carbene as a model for mesityl or diisopropylphenyl substituted NHC ligands. As shown in Table 2 is the NHC ligand in D_{2d} - $\text{Ni}(\text{iPr}_2\text{Im})_2$ much stronger bound ($\Delta E = 50.86$ kcal/mol) as compared to D_{2d} - $\text{Ni}(\text{Ph}_2\text{Im})_2$ ($\Delta E = 44.86$ kcal/mol). This reduction of the overall coordination-bond energy ΔE stems on one hand from increased steric interaction in the case of D_{2d} - $\text{Ni}(\text{Ph}_2\text{Im})_2$, which is reflected in the large preparation energy for the ligand and on the other hand from a decrease in orbital interaction for D_{2d} - $\text{Ni}(\text{Ph}_2\text{Im})_2$. The preparation energy for the ligand mainly arises from a twist of the phenyl substituent of the ligand out of the plane of the imidazole ring into an orthogonal position which is accompanied by a loss of resonance energy (see Fig. 6 for the geometry optimized structures). The orbital interaction energy of D_{2d} - $\text{Ni}(\text{iPr}_2\text{Im})_2$ is slightly larger ($\Delta E_{\text{oi}} = -52.48$ kcal/mol) as compared

to D_{2d} - $\text{Ni}(\text{Ph}_2\text{Im})_2$ ($\Delta E_{\text{oi}} = -50.78$ kcal/mol), which is mainly due to the better σ -interaction in D_{2d} - $\text{Ni}(\text{iPr}_2\text{Im})_2$. In D_{2d} - $\text{Ni}(\text{Ph}_2\text{Im})_2$, σ - and π -contributions are well balanced (–21.52 kcal/mol (σ) vs. –21.76 kcal/mol (π)), whereas in D_{2d} - $\text{Ni}(\text{iPr}_2\text{Im})_2$ the σ -contributions dominate (–25.29 kcal/mol (σ) vs. –19.58 kcal/mol (π)). This means that the ligand iPr₂Im is a better σ -donor and a worse π -acceptor than Ph₂Im and transfers therefore more electron density to the transition metal.

4.5. Effect of metal-complex fragment on M–NHC bonding

We further wanted to systematically vary the nature of the nickel complex fragment ML_n attached to the H_2Im ligand to investigate the influence of the group electronegativity of the complex fragment on Ni–NHC bonding. Experimentally, the substitution reaction involving $[\text{Ni}(\text{CO})_4]$ and NHCs critically depend on the steric properties of the NHC ligand, similar to what has been observed for the reaction of NHCs with $\text{Ni}(\text{COD})_2$. In the case of aryl-substituted carbenes, such as Mes₂Im, Dip₂Im and others, complexes of the type $[\text{Ni}(\text{NHC})(\text{CO})_3]$ are formed. The most bulky NHC ligands *t*Bu₂Im and Ad₂Im (Ad = adamantly),

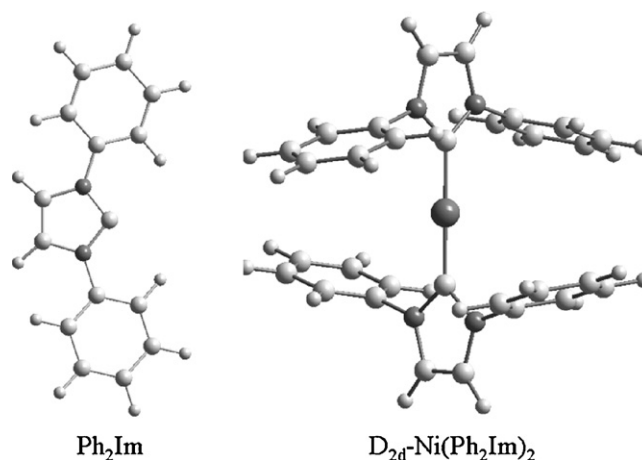


Fig. 6. Optimized structures of Ph_2Im (left side) and D_{2d} - $\text{Ni}(\text{Ph}_2\text{Im})_2$ (right side).

Table 3Metal–carbene bond energy decomposition (in kcal/mol) for complexes $\text{Ni}(\text{H}_2\text{Im})_x(\text{CO})_y$ ^a

	$\text{Ni}(\text{H}_2\text{Im})_3 D_3(C_2)$	$\text{Ni}(\text{H}_2\text{Im})_3 D_{3h}(C_{2v})$	$\text{Ni}(\text{H}_2\text{Im})_2 D_{2d}(C_{2v})$	$\text{Ni}(\text{H}_2\text{Im})_2 D_{2h}(C_{2v})$	$\text{Ni}(\text{H}_2\text{Im})\text{CO } C_{2v}(C_{2v})$	$\text{Ni}(\text{H}_2\text{Im})(\text{CO})_2 C_{2v}(C_{2v})$	$\text{Ni}(\text{H}_2\text{Im})(\text{CO})_3 Cs(Cs)$
Decomposition of orbital interactions ^b							
σ	(−35.55)	−36.01	−21.86	−22.83	−20.63	−30.69	−39.32
A_2		−5.47	−5.75	−7.31	−4.35	−3.02	
π	(−28.46)	−23.17	−20.94	−16.92	−10.71	−11.48	−7.03
ΔE_{oi}	−64.01	−64.65	−48.55	−47.06	−35.69	−44.83	−46.35
% π to ΔE_{oi}	(44.4)	35.8	43.1	35.9	30.0	25.6	15.2
Decomposition of interaction energy ^c							
ΔE_{oi}	−64.01	−64.65	−48.55	−47.06	−35.69	−44.83	−46.35
ΔE_{Pauli}	172.19	171.19	137.81	136.84	103.31	123.88	123.92
ΔV_{elstat}	−145.21	−143.36	−143.46	−142.67	−125.48	−125.38	−118.42
ΔE_{int}	−37.03	−36.82	−54.21	−52.89	−57.86	−46.33	−40.85
Decomposition of overall bond energy ^d							
ΔE_{int}	−37.03	−36.82	−54.21	−52.89	−57.86	−46.33	−40.85
$\Delta E_{\text{prep}}(\text{ML}_n)$	+19.10	+18.70	+2.23	+2.35	+1.08	+7.01	+8.78
$\Delta E_{\text{prep}}(\text{L})$	+0.63	+0.46	+0.39	+0.35	+0.36	+0.28	+0.33
ΔE	−17.30	−17.66	−51.59	−50.19	−56.42	−39.04	−31.74

^a Computed at BLYP/TZ2P.^b $\Delta E_{oi} = \Delta E_{oi}(I_1) + \Delta E_{oi}(I_2) + \dots$ ^c $\Delta E_{\text{int}} = \Delta E_{oi} + \Delta V_{\text{elstat}} + \Delta E_{\text{Pauli}}$.^d $\Delta E = \Delta E_{\text{int}} + \Delta E_{\text{prep}}(\text{ML}_n) + \Delta E_{\text{prep}}(\text{L})$.

however, led to the formation of complexes 16-electron three-coordinate carbonyl nickel compounds $\text{Ni}(\text{NHC})(\text{CO})_2$ [9]. The complexes $\text{Ni}(\text{NHC})_2(\text{CO})_2$ and $\text{Ni}(\text{NHC})(\text{CO})_3$ show the expected tetrahedral geometry at the metal center, the tricarbonyl complexes $\text{Ni}(\text{NHC})(\text{CO})_3$ and dicarbonyl complexes $\text{Ni}(\text{NHC})(\text{CO})_2$ have experimentally observed Ni–C(NHC) bond lengths in a range of 1.95–1.98 Å [9h], which is in good agreement with our optimized geometries.

We systematically varied for our calculations the nature of the nickel complex fragment ML_n by the introduction of carbonyl ligands. The geometry optimized structures for the carbonyl complexes under consideration are depicted in Fig. 3. The results of the bond energy decomposition are summarized in Table 3 and compared to the nickel compounds discussed above. Starting out from the seemingly electron rich $\text{Ni}(\text{H}_2\text{Im})_2$, one of the NHC ligands was replaced to give the (hypothetical) molecule $\text{Ni}(\text{H}_2\text{Im})(\text{CO})$, which adopts a structure with a linear $\text{C}_{\text{carbene}}\text{–Ni–C}_{\text{CO}}$ axis. Analysis of the Ni– $\text{C}_{\text{carbene}}$ bond reveals a drop in π -contribution to 30% (from 43.1% for $D_{2d}\text{–Ni}(\text{H}_2\text{Im})_2$) and an increased importance of electrostatic contributions to Ni–NHC bonding. This trend is continued when increasingly more CO ligands are added to the nickel complex to give $\text{Ni}(\text{H}_2\text{Im})(\text{CO})_2$ (26% π -contribution), and $\text{Ni}(\text{H}_2\text{Im})(\text{CO})_3$ (15% π -contribution). For a proper comparison of the Ni–NHC bonding in three-coordinated complexes $\text{Ni}(\text{H}_2\text{Im})\text{L}_2$ we included calculations on $D_{3h}\text{–Ni}(\text{H}_2\text{Im})_3$, a model for the experimentally observed complex $\text{Ni}(\text{Me}_2\text{Im})_3$ [10b]. According to the energy decomposition scheme, the trends are here the same as observed for the two-coordinated complexes (see Table 3).

Finally, we were interested if there is an electronic reason why the energy minimum for complexes $\text{M}(\text{H}_2\text{Im})_2$ is a slightly twisted, D_{2d} -symmetric structure. There is, of course, also a steric component if the ligands R_2Im get too bulky, but here is also an electronic component for this distortion. The complex $D_{2d}\text{–Ni}(\text{iPr}_2\text{Im})_2$ is only 2.26 kcal/mol lower in energy compared to $D_{2h}\text{–Ni}(\text{iPr}_2\text{Im})_2$. The energy decomposition scheme reveals that the slightly increased overall coordination-bond energy ΔE for the D_{2d} symmetric compound mainly stems from a strengthening (by approximately 4 kcal/mol) in the π orbital interactions.

5. Conclusions

We have shown that π -interactions have to be considered for a proper description of the bonding of NHCs to transition metal atoms. In the case of electron-rich nickel complexes, π -interaction accounts for up to 43% of the total orbital interaction energy ΔE_{oi} . The importance of backbonding to the metal atom critically depends on the nature of the metal (for d^{10} metals $\text{Ni} > \text{Pd} > \text{Pt}$) and the nature/electronic situation of the metal complex fragment. With increasing carbonyl content of our model complexes, π -contributions become less important. This is probably one reason for the picture of NHCs as more or less pure σ -donating ligands developed in the past. Previous theoretical investigations have been mainly performed either on NHC stabilized carbonyl complexes and/or on complexes of 4d and 5d metals, in which π -contributions are less important as compared to 3d metals. TM–NHC bonding has apparently more facets as commonly accepted and the nature of the TM–NHC bonds varies in detail from metal to metal and metal-complex fragment to metal-complex fragment.

Acknowledgements

This work has been performed with the support of the European Union–Research Infrastructure Action under the FP6 “Structuring the European Research Area” Programme (HPC-EUROPA, Project (RII3-CT-2003-506079). We also thank the Fonds der Chemischen Industrie, the Deutsche Forschungsgemeinschaft, and the Netherlands Organization for Scientific Research (NWO–CW and NWO–NCF) and the National Research School Combination–Catalysis (NRSC–C) for financial support. The calculations were carried out on Aster and Huygens parallel machines of the Stichting Academisch Rekencentrum Amsterdam (SARA) and on the TC cluster of the Vrije Universiteit.

References

- [1] (a) H.-W. Wanzlick, H.J. Kleiner, *Angew. Chem.* 73 (1961) 493; (b) H.-W. Wanzlick, *Angew. Chem. Int. Ed. Engl.* 1 (1962) 75; (c) H.-W. Wanzlick, F. Esser, H.J. Kleiner, *J. Chem. Ber.* 96 (1963) 1208.
- [2] (a) A. Berndt, *Angew. Chem. Int. Ed.* 32 (1993) 985; (b) W.A. Herrmann, C. Köcher, *Angew. Chem. Int. Ed.* 36 (1997) 2162;

- (c) D. Bourissou, O. Guerret, F.P. Gabbaï, G. Bertrand, *Chem. Rev.* 100 (2000) 39;
 (d) R.W. Alder, M.E. Blake, L. Chaker, J.N. Harvey, F. Paolini, J. Schütz, *Angew. Chem. Int. Ed.* 43 (2004) 5896;
 (e) F.E. Hahn, *Angew. Chem. Int. Ed.* 45 (2006) 1348.
- [3] (a) A.J. Arduengo, *Acc. Chem. Res.* 32 (1999) 913;
 (b) W.A. Herrmann, *Angew. Chem. Int. Ed.* 41 (2002) 1290;
 (d) N.M. Scott, S.P. Nolan, *Eur. J. Inorg. Chem.* (2005) 1815;
 (e) Special issue: *Coord. Chem. Rev.* 251 (2006) 595 ff;
 (f) F. Glorius (Ed.), *Topics in Organometallic Chemistry 21* (N-heterocyclic Carbenes in Transition Metal Catalysis), Springer, Berlin/Heidelberg, Germany, 2007.
- [4] (a) H. Clavier, K. Grela, A. Kirschning, M. Mauduit, S.P. Nolan, *Angew. Chem., Int. Ed.* 46 (2007) 6786;
 (b) R.H. Grubbs, *Angew. Chem. Int. Ed.* 45 (2006) 3760;
 (c) R.H. Grubbs, *Tetrahedron* 60 (2004) 7117;
 (d) T.M. Trnka, R.H. Grubbs, *Acc. Chem. Res.* 34 (2001) 18.
- [5] (a) E.A.B. Kantchev, C.J. O'Brien, M.G. Organ, *Angew. Chem. Int. Ed.* 46 (2007) 2768;
 (b) S. Díez-González, S.P. Nolan, *Top. Organomet. Chem.* 21 (2007) 47;
 (c) M.R. Netherton, G.C. Fu, *Top. Organomet. Chem.* 14 (2005) 85;
 (d) M.S. Viciu, S.P. Nolan, *Top. Organomet. Chem.* 14 (2005) 241;
 (e) E.A.B. Kantchev, C.J. O'Brien, M.G. Organ, *Aldrichim. Acta* 39 (2006) 97;
 (f) U. Christmann, R. Vilar, *Angew. Chem. Int. Ed.* 44 (2005) 366;
 (g) A.F. Littke, G.C. Fu, *Angew. Chem. Int. Ed.* 41 (2002) 4176.
- [6] (a) M.J. Clarke, H. Taube, *J. Am. Chem. Soc.* 97 (1975) 1397;
 (b) C. Boehme, G. Frenking, *Organometallics* 17 (1998) 5801;
 (c) D.V. Deubel, *Organometallics* 21 (2002) 4303;
 (d) A.T. Termaten, M. Schakel, A.W. Ehlers, M. Lutz, A.L. Spek, K. Lammertsma, *Chem. Eur. J.* 9 (2003) 3577;
 (e) X. Hu, Y. Tang, P. Gantzel, K. Meyer, *Organometallics* 22 (2003) 612;
 (f) X. Hu, I. Castro-Rodriguez, K. Olsen, K. Meyer, *Organometallics* 23 (2004) 755;
 (g) D. Nemcsok, K. Wichmann, G. Frenking, *Organometallics* 23 (2004) 3640;
 (h) N.M. Scott, R. Dorta, E.D. Stevens, A. Correa, L. Cavallo, S.P. Nolan, *J. Am. Chem. Soc.* 127 (2005) 3516;
 (i) G. Frenking, M. Solà, S.F. Vyboishchikov, *J. Organomet. Chem.* 690 (2005) 6178;
 (j) L. Cavallo, A. Correa, C. Costabile, H. Jacobsen, *J. Organomet. Chem.* 690 (2005) 5407;
 (k) H. Jacobsen, A. Correa, C. Costabile, L. Cavallo, *J. Organomet. Chem.* 691 (2006) 4350;
 (l) S.K. Schneider, G.R. Julius, C. Loschen, H.G. Raubenheimer, G. Frenking, W.A. Herrmann, *Dalton Trans.* (2006) 1226;
 (m) A. Kausamo, H.M. Tuononen, K.E. Krahulic, R. Roesler, *Inorg. Chem.* 47 (2008) 1145;
 (n) S. Díez-González, S.P. Nolan, *Coord. Chem. Rev.* 251 (2007) 874;
 (o) R. Tonner, G. Heydenrych, G. Frenking, *Chem. Asian J.* 2 (2007) 1555;
 (p) M.D. Sanderson, J.W. Kamplain, C.W. Bielawski, *J. Am. Chem. Soc.* 128 (2006) 16514;
 (q) D.M. Khranov, V.M. Lynch, C.W. Bielawski, *Organometallics* 26 (2007) 6042;
 R.A. Kelly III, H. Clavier, S. Giudice, N.M. Scott, E.D. Stevens, J. Bordner, I. Samardjiev, C.D. Hoff, L. Cavallo, S.P. Nolan, *Organometallics* 27 (2008) 202.
- [7] (a) D.A. Dixon, A.J. Arduengo, *J. Phys. Chem.* 95 (1991) 4180;
 (b) J. Cioslowski, *Int. J. Quantum Chem.: Quantum Chem. Symp.* 27 (1993) 309;
 (c) C. Heinemann, W. Thiel, *Chem. Phys. Lett.* 217 (1994) 11;
 (d) C. Heinemann, T. Müller, Y. Apeloig, H. Schwarz, *J. Am. Chem. Soc.* 118 (1996) 2023;
 (e) C. Böhme, G. Frenking, *J. Am. Chem. Soc.* 118 (1996) 2039.
- [8] (a) A.J. Arduengo, S. Gamper, J.C. Calabrese, F. Davidson, *J. Am. Chem. Soc.* 116 (1994) 4391;
 (b) V.P.W. Böhm, C.W.K. Gstöttmayr, T. Weskamp, W.A. Herrmann, *Angew. Chem.* 113 (2001) 3500;
 V.P.W. Böhm, C.W.K. Gstöttmayr, T. Weskamp, W.A. Herrmann, *Angew. Chem. Int. Ed.* 40 (2001) 2287;
 (c) P.L. Arnold, F.G.N. Cloke, T. Geldbach, P.B. Hitchcock, *Organometallics* 18 (1999) 3228;
 (d) For similar structurally characterized palladium complexes see: C.W.K. Gstöttmayr, V.P.W. Böhm, E. Herdtweck, M. Grosche, W.A. Herrmann, *Angew. Chem.* 114 (2002) 1421;
 C.W.K. Gstöttmayr, V.P.W. Böhm, E. Herdtweck, M. Grosche, W.A. Herrmann, *Angew. Chem. Int. Ed.* 41 (2002) 1363;
 (e) M.M. Konnick, I.A. Guzei, S.S. Stahl, *J. Am. Chem. Soc.* 126 (2004) 10212;
 (f) M. Yamashita, K. Goto, T. Kawashima, *J. Am. Chem. Soc.* 127 (2005) 7294.
- [9] See, for example:
 (a) K. Ofele, W.A. Herrmann, D. Mihalios, M. Elison, E. Herdtweck, W. Scherer, J. Mink, *J. Organomet. Chem.* 459 (1993) 177;
 (b) W.A. Herrmann, M. Elison, J. Fischer, C. Kocher, G.R. Artus, *Angew. Chem. Int. Ed. Engl.* 34 (1995) 2371;
 (c) W.A. Herrmann, L.J. Goossen, G.R.J. Artus, C. Köcher, *Organometallics* 16 (1997) 2472;
 (d) T. Weskamp, F.J. Kohl, W. Hieringer, D. Gleich, W.A. Herrmann, *Angew. Chem. Int. Ed.* 38 (1999) 2416;
 (e) J. Schwarz, V.P.W. Böhm, M.G. Gardiner, M. Grosche, W.A. Herrmann, W. Hieringer, G. Raudaschl-Sieber, *Chem. Eur. J.* 6 (2000) 1773;
 (f) R. Dorta, E.D. Stevens, C.D. Hoff, S.P. Nolan, *J. Am. Chem. Soc.* 125 (2003) 10490;
 (g) M.-T. Lee, C.-H. Hu, *Organometallics* 23 (2004) 976;
 (h) R. Dorta, E.D. Stevens, N.M. Scott, C. Costabile, L. Cavallo, C.D. Hoff, S.P. Nolan, *J. Am. Chem. Soc.* 127 (2005) 2485.
- [10] (a) T. Schaub, U. Radius, *Chem. Eur. J.* 11 (2005) 5024;
 (b) T. Schaub, M. Backes, U. Radius, *Organometallics* 25 (2006) 4196;
 (c) T. Schaub, M. Backes, U. Radius, *J. Am. Chem. Soc.* 128 (2006) 15964;
 (d) T. Schaub, U. Radius, *Z. Anorg. Allg. Chem.* 632 (2006) 981;
 (e) T. Schaub, C. Döring, U. Radius, *Dalton Trans.* (2007) 1993;
 (f) T. Schaub, M. Backes, U. Radius, *Chem. Commun.* (2007) 2037;
 (g) T. Schaub, U. Radius, *Z. Anorg. Allg. Chem.* 633 (2007) 2168.
- [11] (a) P. Hohenberg, W. Kohn, *Phys. Rev.* 136 (1964) B864;
 (b) W. Kohn, L.J. Sham, *Phys. Rev.* 140 (1965) A1133;
 (c) R.G. Parr, W. Yang, *Density-Functional Theory of Atoms and Molecules*, Oxford University Press, New York, 1989.
- [12] (a) G. te Velde, F.M. Bickelhaupt, E.J. Baerends, C. Fonseca Guerra, S.J.A. van Gisbergen, J.G. Snijders, T. Ziegler, *J. Comput. Chem.* 22 (2001) 931;
 (b) E.J. Baerends, D.E. Ellis, P. Ros, *Chem. Phys.* 2 (1973) 41.
- [13] Computer code ADF2007.01: E.J. Baerends, J. Autschbach, A. Bérces, J.A. Berger, F.M. Bickelhaupt, C. Bo, P.L. de Boei, P.M. Boerrigter, L. Cavallo, D.P. Chong, L. Deng, R.M. Dickson, D.E. Ellis, M. van Faassen, L. Fan, T.H. Fischer, C. Fonseca Guerra, S.J.A. van Gisbergen, J.A. Groeneveld, O.V. Gritsenko, M. Grüning, F.E. Harris, P. van den Hoek, C.R. Jacob, H. Jacobsen, L. Jensen, E.S. Kadantsev, G. van Kessel, R. Klooster, F. Kootstra, E. van Lenthe, D.A. McCormack, A. Michalak, J. Neugebauer, V.P. Nicu, V.P. Osinga, S. Patchkovskii, P.H.T. Philipsen, D. Post, C.C. Pye, W. Ravenek, P. Romaniello, P. Ros, P.R.T. Schipper, G. Schreckenbach, J.G. Snijders, M. Solà, M. Swart, D. Swerhone, G. te Velde, P. Vernooijs, L. Versluis, L. Visscher, O. Visser, F. Wang, T.A. Wesolowski, E.M. van Wezenbeek, G. Wiesenekker, S.K. Wolff, T.K. Woo, A.L. Yakovlev, T. Ziegler, *Scientific Computing & Modeling, Theoretical Chemistry*, Vrije Universiteit, Amsterdam, The Netherlands, 2007.
- [14] (a) A.D. Becke, *Phys. Rev. A* 38 (1988) 3098;
 (b) C. Lee, W. Yang, R.G. Parr, *Phys. Rev. B* 37 (1988) 785.
- [15] E. van Lenthe, E.J. Baerends, J.G. Snijders, *J. Chem. Phys.* 101 (1994) 9783.
- [16] (a) G.Th. de Jong, M. Solà, L. Visscher, F.M. Bickelhaupt, *J. Chem. Phys.* 121 (2004) 9982;
 (b) G.Th. de Jong, D.P. Geerke, A. Diefenbach, F.M. Bickelhaupt, *Chem. Phys.* 313 (2005) 261;
 (c) G.Th. de Jong, D.P. Geerke, A. Diefenbach, M. Solà, F.M. Bickelhaupt, *J. Comput. Chem.* 26 (2005) 1006;
 (d) G.Th. de Jong, F.M. Bickelhaupt, *J. Phys. Chem. A* 109 (2005) 9685;
 (e) G.Th. de Jong, F.M. Bickelhaupt, *J. Chem. Theory Comput.* 2 (2006) 322.
- [17] (a) F.M. Bickelhaupt, E.J. Baerends, In: K.B. Lipkowitz, D.B. Boyd, (Eds.), *Rev. Comput. Chem.*, vol. 15, Wiley-VCH, New York, 2000, p. 1;
 See also:
 (b) F.M. Bickelhaupt, N.M.M. Nibbering, E.M. van Wezenbeek, E.J. Baerends, *J. Phys. Chem.* 96 (1992) 4864;
 (c) F.M. Bickelhaupt, A. Diefenbach, S.P. de Visser, L.J. de Koning, N.M.M. Nibbering, *J. Phys. Chem. A* 102 (1998) 9549.
- [18] (a) T. Ziegler, A. Rauk, *Inorg. Chem.* 18 (1979) 1755;
 (b) T. Ziegler, A. Rauk, *Inorg. Chem.* 18 (1979) 1558;
 (c) T. Ziegler, A. Rauk, *Theor. Chim. Acta* 46 (1977) 1.
- [19] K. Morokuma, *Acc. Chem. Res.* 10 (1977) 294.
- [20] (a) C. Fonseca Guerra, J.-W. Handgraaf, E.J. Baerends, F.M. Bickelhaupt, *J. Comput. Chem.* 25 (2004) 189;
 (b) F.M. Bickelhaupt, N.J.R. van Eikema Hommes, C. Fonseca Guerra, E.J. Baerends, *Organometallics* 15 (1996) 2923.
- [21] (a) G.F. Voronoi, *Z. Reine, Angew. Math.* 134 (1908) 198;
 (b) C. Kittel, *Introduction to Solid State Physics*, Wiley, New York, 1986.
- [22] (a) A.J. Arduengo, R.L. Harlow, M. Kline, *J. Am. Chem. Soc.* 113 (1991) 361.
- [23] (a) U. Radius, F.M. Bickelhaupt, A.W. Ehlers, N. Goldberg, R. Hoffmann, *Inorg. Chem.* 37 (1998) 1080;
 (b) A.W. Ehlers, E.J. Baerends, F.M. Bickelhaupt, U. Radius, *Chem. Eur. J.* 4 (1998) 210;
 (c) F.M. Bickelhaupt, U. Radius, A.W. Ehlers, R. Hoffmann, E.J. Baerends, *New. J. Chem.* (1998) 1.
- [24] V.M. Rayon, G. Frenking, *Organometallics* 22 (2003) 3304.
- [25] K. Fukui, *Angew. Chem. Int. Ed. Engl.* 21 (1982) 801.
- [26] See, for example:
 (a) T. Ziegler, J. Autschbach, *Chem. Rev.* 105 (2005) 695;
 (b) J. Li, T. Ziegler, *Organometallics* 15 (1996) 3844;
 (c) S. Dapprich, G. Frenking, *Angew. Chem. Int. Ed. Engl.* 34 (1995) 354.